

An Assessment of Future Dryness over Korea Based on the ECHAM5-RegCM3 Model Chain under A1B Emission Scenario

Eun-Soon Im¹, Joong-Bae Ahn², and Do-Woo Kim¹

¹National Institute of Meteorological Research, Korea Meteorological Administration, Seoul, Korea

²Department of Atmospheric Sciences, Pusan National University, Busan, Korea

(Manuscript received 23 September 2011; revised 8 January 2012; accepted 5 February 2012)
© The Korean Meteorological Society and Springer 2012

Abstract: We analyze the future dryness over Korea based on the projected temperature and precipitation. For fine-scale climate information, the ECHAM5/MPI-OM A1B simulation has been dynamically downscaled using the RegCM3 double-nested system. A 130-year long-term climatology (1971–2100) from the mother domain (East Asia: 60 km) and nested domain (South Korea: 20 km) is discussed. Based on the intercomparison with CMIP3 participant models, the ECHAM5/MPI-OM provides climatic change information over the East Asia that is not markedly different from other projections. However, the reduction of summer precipitation over Korea is rather different with ensemble mean of CMIP3 participant models. The downscaled results generally follow the behavior of ECHAM5/MPI-OM, but substantial fine-scale details are found in the spatial pattern and the change signals become more enhanced at the local scale. In the future projection, significant warming is found regardless of the season and region while the change in precipitation shows a mixed feature with both increasing and decreasing patterns. The increase of temperature enhances the evapotranspiration, and hence the actual water stress becomes more pronounced in the warmer climate. This is related to the negative trends of the self-calibrating Palmer Drought Severity Index (PDSI) to measure the drought condition in Korea. Although PDSI is overall associated with the precipitation variation, its long-term trend tends to be modulated by the temperature trend. It is confirmed that the detrended temperature is shown to mask the decreasing tendency of the PDSI. The result indicates that without an increase in precipitation appropriate for atmospheric moisture demand, future dryness is a more likely condition under global warming.

Key words: Future dryness, global warming, dynamical downscaling, ECHAM5-RegCM3

1. Introduction

There is a growing agreement of the broad increase of precipitation over East Asia under global warming based on climate change projections with global climate models (GCMs; IPCC, 2007). Kripalani *et al.* (2007) reported that the multi-model ensemble from 19 coupled climate models in the IPCC AR4 database projects a significant increase of summer monsoon

precipitation over East Asia in response to a doubled CO₂ scenario. Kim and Byun (2009) also pointed out using 15 GCMs ensemble that increases in the mean and variability of precipitation are expected under the warming scenario over North and East Asia, and that precipitation changes are directly translated into weakening of drought. However, large quantitative differences among the models remain, and substantial discrepancies arise at the regional scale. Although the GCMs provide the foundation for future climate projections with improved confidence (IPCC, 2007), precipitation projections at the local or regional levels could lead to fairly different interpretations of the results due to large spatial and temporal deviations, which makes it difficult to arrive at any general conclusions. Gao *et al.* (2008) claimed that the climate change signal over East Asia may exhibit a complex spatial structure which can be simulated only with high resolution modeling systems because of complex topography and the unique climate systems of the region. The downscaled regional climate projection of Gao *et al.* (2008) indicates a reduced future monsoon precipitation over China, which is rather different from previous projections over the region.

The Korean peninsula appears to be a particularly representative region that can reveal the limitation of the GCM simulations (Im *et al.*, 2006). South Korea is located at the eastern edge of the huge Asia continent. The geographical area is relatively small and has a complicated mountainous terrain (Im *et al.*, 2007). These physiographical characteristics have a significant effect on weather and climate, thereby highlighting the necessity of the fine-scale climate information for the accurate assessment of future climate. Indeed, even a minor shift in the location and track of the precipitation band from the coarse-grid GCM simulation might result in large errors over the Korean peninsula (Im *et al.*, 2006). For instance, Fig. 1 clearly explains how the representation of topography over narrow peninsula depends critically on the model resolution. The GCMs (Figs. 1a and 1b) hardly show any mountains slopes in the Korean peninsula. Even the low resolution GCM ($4 \times 5^\circ$) represents the southern part of Korean as an ocean grid point. Unrealistic land-sea distribution around Korean peninsula could lead to inaccurate simulation of East Asia summer precipitation (Cha *et al.*, 2007).

In this study, we investigate the potential changes in tempera-

Corresponding Author: Eun-Soon Im, National Institute of Meteorological Research, Korea Meteorological Administration, 250-3 San, Bangdong-ri Sacheon-myeon, Gangneung-si, Gangwon-do 250-852, Korea.

E-mail: esim@korea.kr

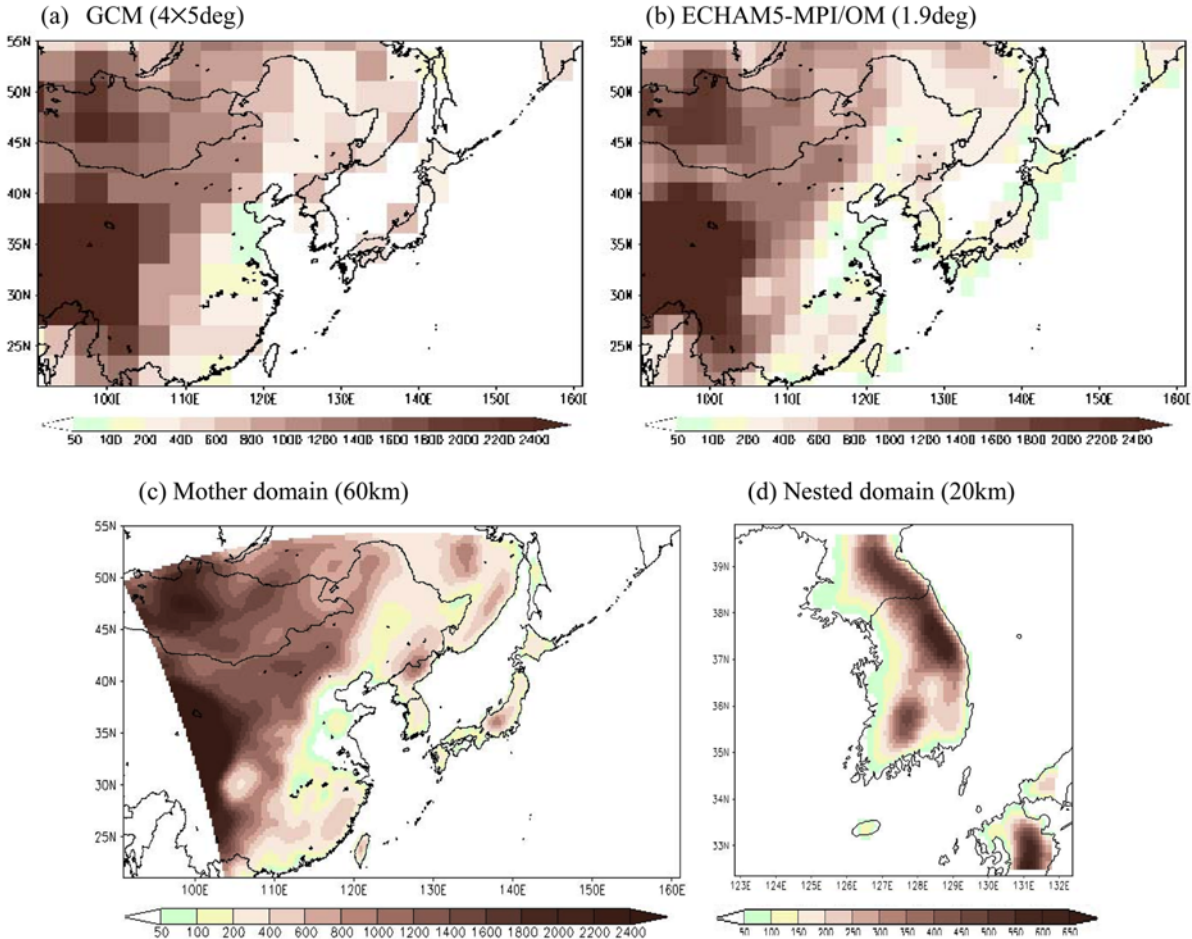


Fig. 1. Representation of the East Asian and Korean peninsula topography at a grid spacing of (a) 4×5 deg (AOGCM from CMIP3), (b) 1.9 deg (ECHAM5-MPI/OM), (c) 60 km (RegCM3 mother domain), and (d) 20 km (RegCM3 nested domain).

ture and precipitation characteristics under global warming and their influences on future dryness using a regional climate projection with a focus on the Korean peninsula. To simulate climate information with a suitably fine-scale for reflecting the local climate characteristics over Korea, we have developed a one-way double-nested regional climate model system (Im *et al.*, 2006). Using this modeling system, we perform a dynamical downscaling of the ECHAM5/MPI-OM climate model under the SRES A1B emission forcing covering the period of 1971–2100 (Im and Ahn, 2011; Im *et al.*, 2011).

First, we assess the uncertainty of the ECHAM5/MPI-OM projection used as the initial and boundary forcing for the RegCM3 downscaling system via an intercomparison with the CMIP3 global model projections. Since this study is based on a single realization – one emission forcing (A1B), one GCM (ECHAM5/MPI-OM) and one RCM (RegCM3), it is important to address the reliability of the ECHAM5/MPI-OM projection. We then consider the RegCM3 downscaled results dealing with both the present climate performance and the potential future changes. We examine the basic features of the mother domain simulation over East Asia, and subsequently the focus moves to the high resolution nested domain simulation over

Korea. Analysis is primarily centered on surface air temperature and precipitation, the two variables most used in impact assessment studies. Changes in temperature and precipitation patterns are expected in an altered moisture budget. As for the effective indication of water imbalance in atmospheric moisture supply and demand at the surface, we compute the self-calibrating Palmer Drought Severity Index (PDSI) (Wells *et al.*, 2004). The PDSI is an index for measuring long-term cumulative meteorological drought condition from precipitation, surface air temperature, and available water content (Andreadis and Lettenmaier, 2006; Dubrovsky *et al.*, 2008; Karnauskas *et al.*, 2008). Since the PDSI incorporates both precipitation and temperature in contrast to many other drought indices that are based on precipitation alone (Dai *et al.*, 2004; Easterling *et al.*, 2007), it is advantageous in quantifying the direct attribution of dryness change to increased emission forcing. To assess the influence of the increasing temperature trend on drought intensity and trend, two sets of PDSI are calculated using different inputs: (1) the projected precipitation and temperature, and (2) the same as precipitation but detrended temperature. By such a comparison, we can enhance our understanding of the relative contribution and role of increasing temperature to

future dryness under global warming.

In section 2, we present a brief description of the modeling system, main analysis methods, and observational dataset. The uncertainty of the ECHAM5-MPI/OM projection, and the validated and projected results for the mother and nested domain simulations are discussed in section 3. The summary and discussion follow in section 4.

2. Data and methods

a. Regional climate model and experiment design

The regional climate model used in this study is the latest version of the International Centre for Theoretical Physics (ICTP) regional climate model, RegCM3 (Pal *et al.*, 2007). The one-way double-nested technique and model configuration applied to this work are the same as those used by Im *et al.* (2011). Briefly, in the RegCM3 double-nested system, the mother domain (Fig. 1c) covers East Asia at 60 km grid spacing (94×80 grid points, including the buffer area) while the nested domain (Fig. 1d) focuses on the South Korean peninsula at 20 km grid spacing (54×54 grid points, including the buffer area). The physical parameterizations employed in this simulation include the comprehensive radiative transfer package of the NCAR Community Climate Model, version CCM3 (Kiehl *et al.*, 1996), the non-local boundary layer scheme of Holtslag *et al.* (1990), the BATS land surface scheme (Dickinson *et al.*, 1993), and the MIT-Emanuel convection scheme (Emanuel, 1991). Intensive validation of present climate reproduction (Im *et al.*, 2006) and climate change simulation (Im *et al.*, 2007) reveals that the RegCM3 nesting system shows encouraging performance in simulating well both climatological and regional characteristics over Korea. In our experiment, the initial and time-dependent meteorological lateral boundary conditions for the mother domain simulation are interpolated at 6-hourly intervals from an ECHAM5/MPI-OM A1B scenario simulation. The ECHAM5/MPI-OM is a coupled atmosphere (ECHAM5)-ocean(MPI-OM) global climate model that was developed by the Max-Planck-Institute for Meteorology (hereafter referred to as ECHAM5). It is the stat-of-the-art coupled global climate model, which was used to conduct ensemble simulations for the fourth assessment report of the IPCC (AR4), and to be successfully downscaled over the European region (e.g., Hagemann *et al.*, 2008). Integration continuously spans the 130-year, consisting of one for present day conditions as a reference (covering the period 1971-2000: 30-year) and one for future climate conditions (covering the period 2001-2100: 100-year). Both the global and regional climate models are described by Im *et al.* (2006, 2011) in detail and the references therein.

b. Analysis methods

To address the issue of future dryness over Korea, the self-calibrating PDSI is calculated using the program of Wells *et al.* (2004) (source code was downloaded from <http://greenleaf.unl.edu/downloads>).

The self-calibrating PDSI is the modified PDSI to account for the expected variability of precipitation between locations by automatically adjusting the climatic characteristic and calculating the duration factors based on the characteristics of the climate at a given location. As a result, the index performs more consistently and allows for more accurate comparisons of the index at different locations. Further details and comparison between the PDSI and self-calibrating PDSI appear in work by Wells *et al.* (2004). Monthly temperature and precipitation are used as input data for the calculation of self-calibrating PDSI. Additionally, the available water holding capacity (AWC) is assigned the same value (100 mm) as adopted by Boo *et al.* (2004) in their use of the algorithm for the Korea Meteorological Administration (KMA). Hereafter, PDSI denotes the results from the self-calibrating PDSI.

c. Observation data

To validate the surface variable (e.g., temperature and precipitation) from the mother domain simulation, we use the global observation dataset of the Climate Research Unit (CRU) of the University of East Anglia (New *et al.*, 2000). The resolution of CRU is 0.5 degree \times 0.5 degree, and we use the 30-year climatology for the same period as the reference simulation (1971-2000). Regarding the nested domain simulation, we use the climate observations from 57 stations maintained by the KMA for the period from 1975 to 2004 throughout the southern part of Korea (see Fig. 1 in Im and Ahn, 2011). Since the number of observational station has been increased since 1974, the period of station observation (1975-2004) is not exactly the same as that of the reference simulation (1971-2000). We compare the results of the nested domain simulation (20 km) with 57 individual station values using the grid points closest to the stations. The relatively high model resolution justifies the comparison between the station data and model data at the grid point closest to the station location (Im *et al.*, 2008b). This dataset allows a first-order validation of the fine-scale structure of the nested domain simulation.

3. Results

a. Uncertainty of the ECHAM5 projection

The realism of any SRES emission scenario, GCM, and RCM simulation can be questioned due to various uncertainty sources. Therefore, large ensembles of experiments comprising multiple forcing scenarios, model configurations, initial conditions, and downscaling approaches would be required to reduce the uncertainty range (Giorgi *et al.*, 2009). However, fine-mesh ensemble scenarios throughout the dynamical downscaling require tons of computer resources. Furthermore, no systematic collaboration for regional climate change projections (e.g., European ENSEMBLES project) has been conducted over our study region, resulting in lacking of downscaling scenarios with a focus on the Korean peninsula. Considering this current

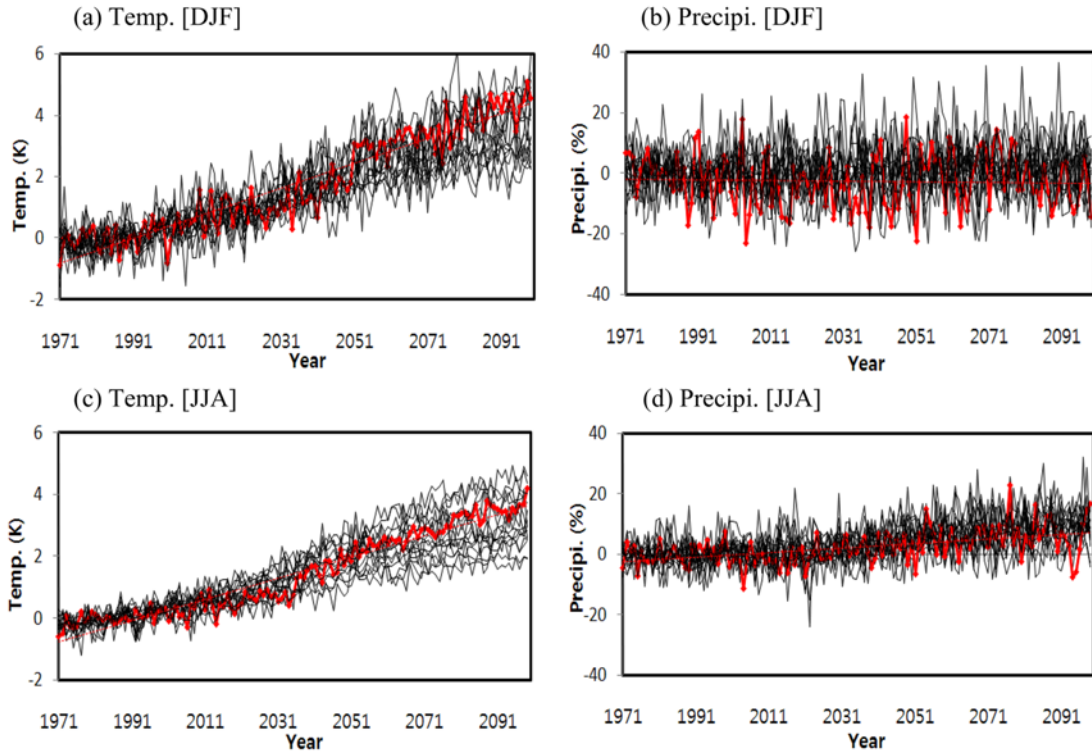


Fig. 2. Temporal evolution of temperature and precipitation anomalies averaged over East Asia (100-150E, 20-50N) from 17 AOGCMs participating in the CMIP3 A1B projections. Here, the thick red line indicates the results from ECHAM5-MPI/OM projection.

circumstance, we started to analyze the Korean scenario simulation from the ECHAM5 and RegCM3 model chain, even though a single realization limits the robustness of the result because of its dependence on the selected projection. It is noted that our objective is not to confirm the future climate condition, but rather to interpret potential change behavior due to emission forcing and to extend our understanding of possible warming effect in the Korean future dryness. Further study should be expanded with multi-model ensembles to derive a more robust statement.

As an attempt to justify the use of one GCM, we investigate the reliability of the ECHAM5 projection by assessing inter-model variability. Figure 2 displays the temporal evolution of the seasonal mean (DJF and JJA) temperature and precipitation anomalies averaged over East Asia from 17 AOGCMs participating in the CMIP3 A1B projections (including ECHAM5). Anomalies are computed by subtracting the average for the reference period (1971-2000). See Coppola and Giorgi (2009) for a detailed GCM description and list of ensemble members (Table 1 in Coppola and Giorgi, 2009). In case of ECHAM5, three ensemble members have been simulated with different initial conditions under the A1B scenario. In this study, the third member is used as the initial and boundary condition for the downscaling. Based on the comparison among the three members, there is not much difference between them (See Fig. 8 in Im *et al.*, 2011). Therefore, a downscaling result of one member may not introduce a significant discrepancy from the ensemble mean of ECHAM5.

For temperature, all models project a coherent increase and the rate of this increase is enhanced in the late 21st century in response to increasing greenhouse gas (GHG) concentration, in spite of the different magnitudes. The behaviors from the ECHAM5 (thick red line) are not markedly different from the other projections, without any deviation from the upper and lower boundaries that are formed by other simulations. On the other hand, changes in precipitation do not show any well-defined regular trend. Only summer precipitation reveals a slightly increase, but natural variability appears to exceed this linear trend. Despite the model dependency of distinct inter- and multi-decadal variations, the precipitation evolution of ECHAM5 is not placed out of the range compared to the other projections.

However, the area-averaged pattern across a relatively broad region could not represent the regional diversity in terms of spatial details. To investigate this issue, we examine the spatial pattern of summer precipitation, which is characterized by dominant regional variability. Figure 3 shows the spatial distribution of summer precipitation change (2071-2100 minus 1971-2000) from the GCM projections. The left, middle, and right panels are from ECHAM5, average of three GCMs (ECHAM5, CNRM, CSIRO), and average of 17 CMIP3 participant GCMs, respectively. Among the 17 GCMs, we select the three GCMs (including ECHAM5) with the relatively high resolution (1.9°). For the regional average, all cases project a precipitation increase (a: 4.74%, b: 4.98%, c: 8.73%), although the spatial distribution is quite different. All ensemble average projects a

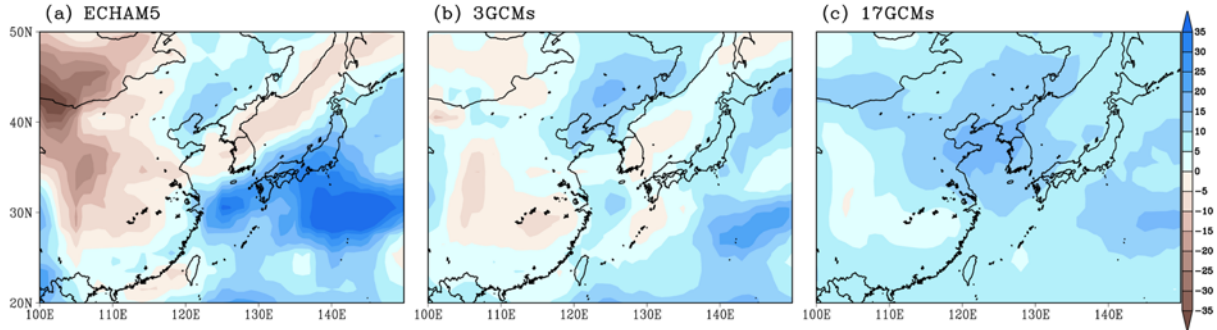


Fig. 3. Spatial distribution of precipitation changes (2071-2100 minus 1971-2000, %) for summer from GCM projections. Here, left, middle, and right panels are from the ECHAM5, 3-GCM average (ECHAM5, CNRM, CSIRO), and 17-GCM average, respectively.

precipitation increase across the whole area whereas ECHAM5 exhibits a broad decrease over mostly land area. The maximum negative region occurs in the northwest China and Mongolia region; however, these regions are characterized by less precipitation, which tend to inflate the percentage. Another main discrepancy is found over Korea. The reduced summer precipitation of ECHAM5 contrasts with the 17 GCMs ensemble average. In fact, there is a large possibility of misinterpretation in trying to derive any consensus of precipitation change from the GCM projections over a narrow peninsula such as Korea. As seen in Fig. 1, some GCMs with relatively low resolution ($4 \times 5^\circ$) prescribe the southern part of Korea as an ocean. Such an unrealistic land-sea distribution cannot accurately simulate the regional precipitation. Even though the magnitude and region of reduced precipitation from the 3-GCM average do not exactly coincide with those of ECHAM5, the negative areas are more expanded mostly over the land compared to the

all ensemble average pattern. At least, none of the three GCMs shows a positive sign over the southern part of Korea in contrast to the pattern from the 17-GCM average (not shown). This suggests that the model resolution can play a critical role in determining the spatial distribution of the variables characterized by dominant regional dependency (e.g., precipitation). This comparison is not intended to provide a quantitative assessment of the effect of resolution of GCMs but it is simply aimed to investigate the different behavior of GCM projections and to understand the characteristics of ECHAM5 in our target area.

b. Changes in temperature and precipitation over East Asia from the mother domain simulation

While considering these general features of ECHAM5, we turn our attention to the detailed spatial and temporal structure

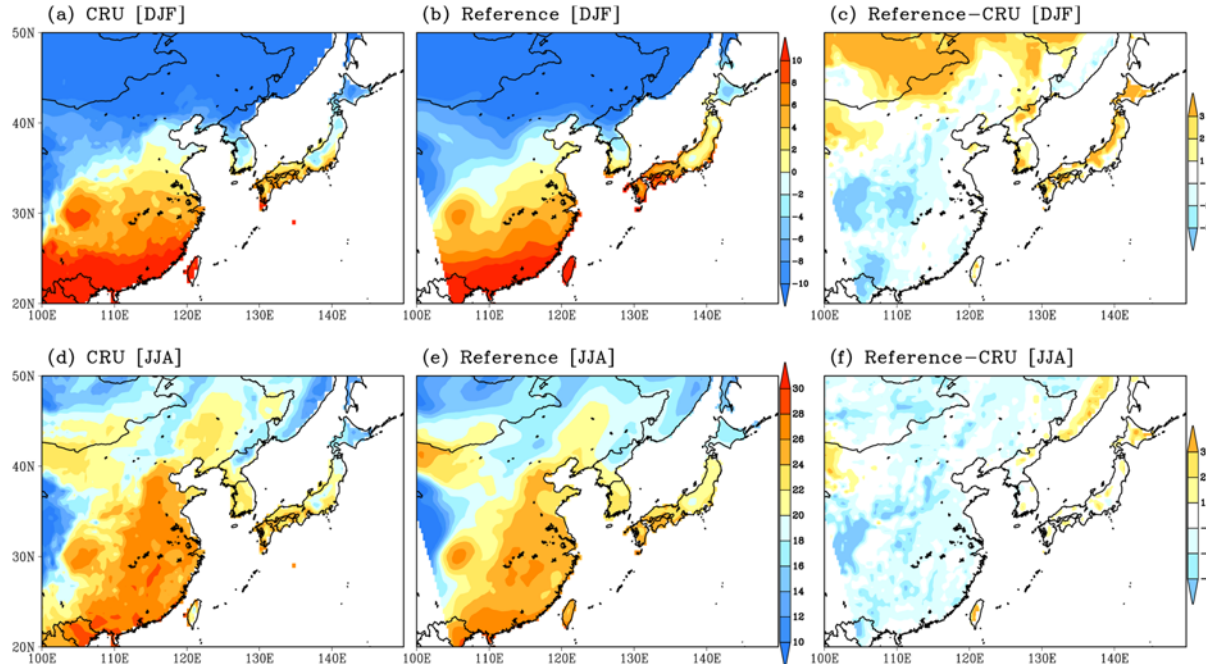


Fig. 4. Surface air temperature of the observation (CRU; a and d), the reference simulation (b and e) and their differences (c and f) for the winter and summer seasons. Units are $^{\circ}\text{C}$.

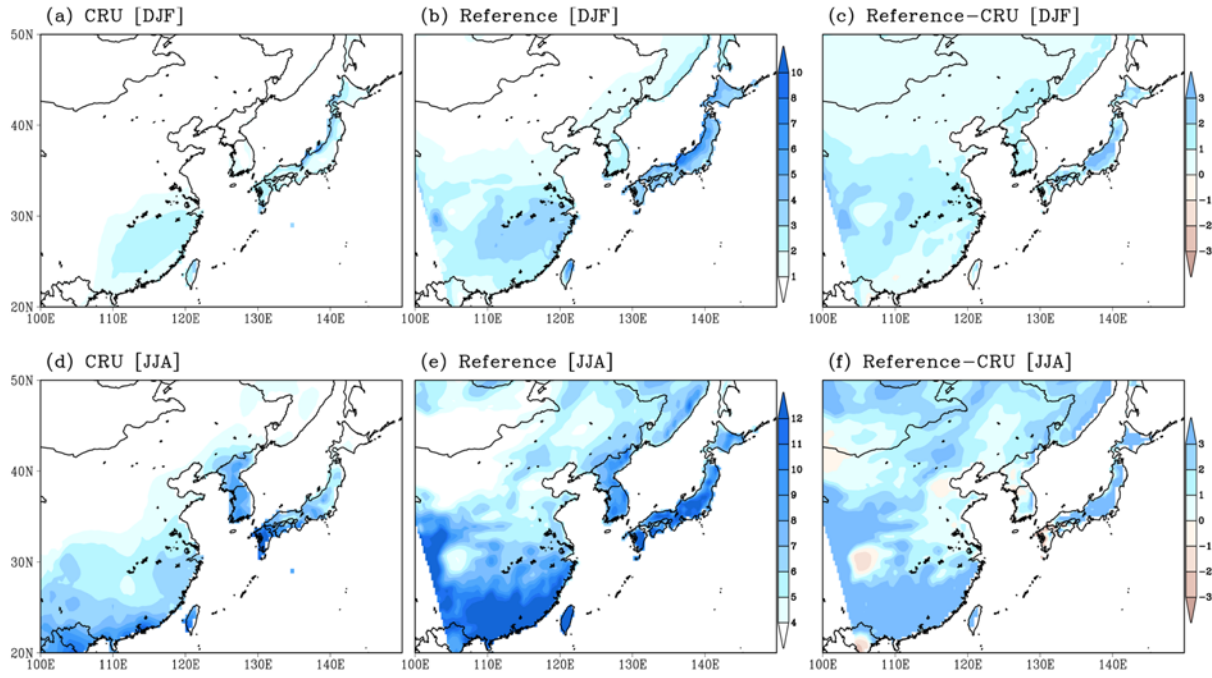


Fig. 5. Precipitation of the observation (CRU; a and d) and reference simulation (b and e) and their differences (c and f) for the winter and summer seasons. Units are mm d^{-1} .

of the downscaled results. At first, we present the temperature and precipitation performance from the mother domain simulation during the reference period. The confidence gained from reference simulation could add to the reliability of our interpretation of the results from the future projection.

Figure 4 presents the spatial distribution of seasonal mean temperature derived from the observation (CRU), the mother domain simulation, and their differences during the reference period for the winter (DJF) and summer (JJA) seasons. The model shows a good agreement with the observation in both seasonality and spatial details. For the summer season, negative biases are dominant, mostly ranging within 2°C . On the other hand, the winter temperature exhibits warm biases in the northern parts and cold biases in the southern parts.

Figure 5 is the same as Fig. 4 except for precipitation. The simulated precipitation fields also reasonably reproduce the observed large scale features and capture the seasonal variation of the precipitation pattern associated with the East Asia monsoon system. The spatial pattern correlations between the simulation and observation are 0.86 in winter and 0.77 in summer. In particular, this summer season performance is comparative with the simulation using the NCEP/NCAR Reanalysis as a boundary condition, as reported by Park *et al.* (2008). However, the model tends to overestimate precipitation over the whole domain. Large errors occur in southeast China in the summer season, in line with those found in other Asian summer monsoon experiments (e.g., Chow *et al.*, 2006). Although the MIT-Emanuel convection scheme used in this experiment considerably improves the precipitation performance over our study region compared to using the Grell convection scheme

(Im *et al.*, 2008b), it usually tends to overestimate the convective precipitation in regions with high SST and water vapor (Chow *et al.*, 2006).

Figure 6 presents the spatial distribution of temperature and precipitation change between the future (2071-2100) and reference (1971-2000) periods of the mother domain simulation for the winter (DJF) and summer (JJA). Future change behaviors show a seasonal dependence in both temperature and precipitation. Even though the temperature is projected to increase regardless of the season, the spatial patterns of the winter and summer distributions are quite different. In winter there tends to be a positive northward gradient with the maximum over the northern area of the Korean peninsula, whereas in summer there tends to be a rather zonal gradient with maximum warming occurring in the northwest China and the Mongolia region which is characterized by less precipitation (see Fig. 5e). Winter warming amplification in the cold climate regimes (e.g., high latitude) has been attributed, at least partially, due to a reduction in snow and the associated snow-albedo feedback mechanism (Im *et al.*, 2008a). This seasonality of temperature change shows a general consistency with the results found in the regional climate projections presented in IPCC (2007, Chapter 11).

In contrast to the temperature, the changes in precipitation show pronounced regional differences with a mixed signal between increasing and decreasing patterns. Even for the 30-year average, the precipitation change pattern in the regional model exhibits a much greater fine scale structure. Compared to ECHAM5 (for summer, Fig. 3a), the general patterns are similar, but spatial details due to the local process appear to be

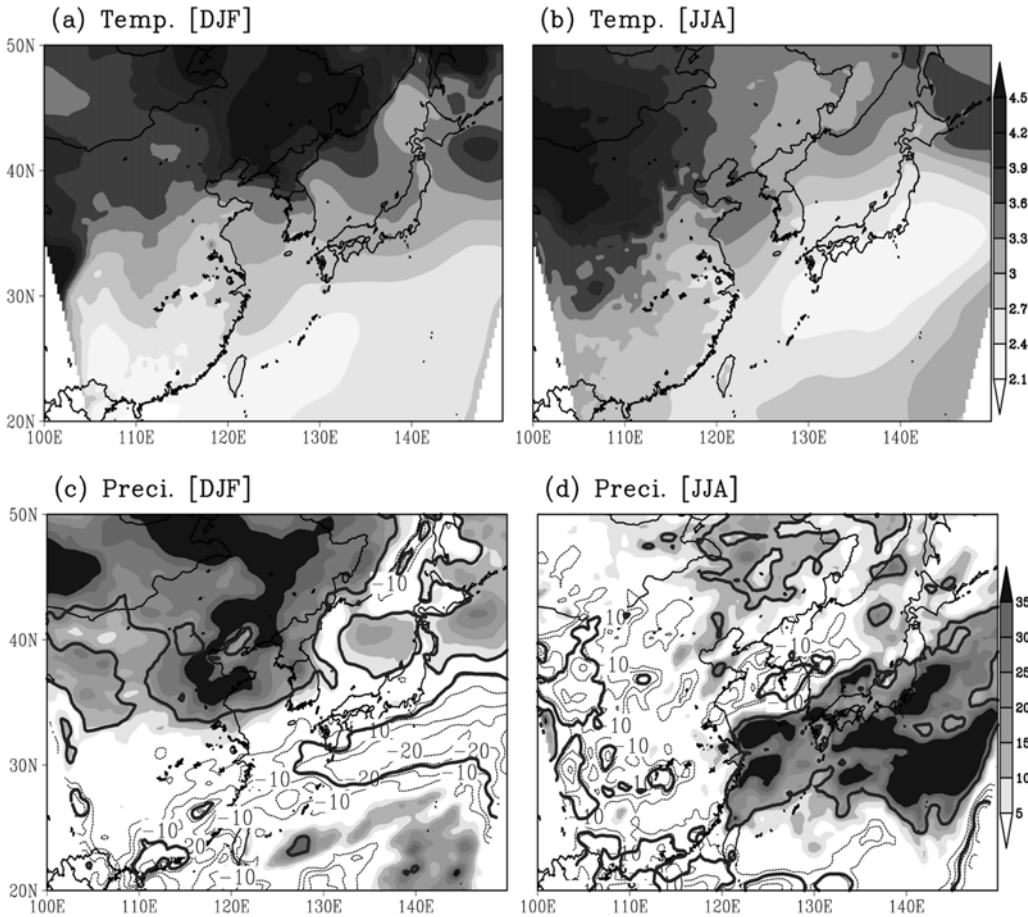


Fig. 6. Surface air temperature (a and b) and precipitation (c and d) changes between the future (2071-2100) and reference (1971-2000) periods of the mother domain simulation over East Asia for the winter (DJF) and summer (JJA) seasons. Units are $^{\circ}\text{C}$ (temperature) and % (precipitation). Thick line in precipitation indicates areas where the change is statistically significant at the 90% confidence level.

mostly smoothed or eliminated in the coarse-grid GCM simulations. Hence, the downscaled results tend to enhance the change signal at the local scale. Influences of the natural variability should also be larger in higher resolution RCM than in GCM. The decreased precipitation over Korea was also enhanced slightly. However, there is an exception that the negative signals in Mongolia disappeared in the regional model result. This result needs to be examined in detail in future studies. For winter, a widespread increase in precipitation is observed over the northeastern part of Asia continent (including the Korean peninsula). At the same time, there are the localized negative areas mostly over the ocean and south China region. The change signal of summer precipitation is mixed and complicated as well. Nevertheless, when looking at the regional average, increases in precipitation for both seasons are evident (DJF: 8.2% and JJA: 6.6%), which is consistent with the GCM projections reported by recent publications (e.g., IPCC, 2007; Kripalani *et al.*, 2007).

To diagnose the statistical significance of the projected changes, we carried out a two-tailed t-test for the temperature and precipitation (Fig. 6). The temperature changes are statistically significant at the 90% confidence level in all seasons

and over the entire region (not indicated by the line). For the precipitation change, the statistically significant regions are restricted to some parts of the simulated area, and spatial patterns are very complicated in correspondence of the precipitation variability. While the significant increase of winter precipitation is observed over northeastern Asia, a significant increase of summer precipitation is observed over the south sea of Korea and Japan.

c. Changes in drought over Korea from the nested domain simulation

In order to justify the use of the double nesting approach, we assess the quality of the simulated results for the nested domain via comparison with the mother domain results and ECHAM5 driving field over the nested domain area as reference. Figure 7 presents the spatial distribution of precipitation averaged over the 30-year reference period (OBS: 1975-2004, Model: 1971-2000) for the winter (DJF) and summer (JJA) seasons. The first column shows the observation fields obtained from the 57 station dataset. The second column shows the nested domain results, while the third presents the results from the

mother domain simulations over the nested domain area. Finally, the fourth column shows the results from the ECHAM5 driving GCM as the reference. Therefore, we assess the quality of the simulated results across different spatial scales, and how a high resolution can improve the accuracy of the climatological feature. First of all, the results clearly show the scale dependency in both winter and summer. ECHAM5 overestimates the winter precipitation and underestimates the summer precipitation, and entirely fails to capture the spatial variability. On the other hand, the nested domain results are mostly closer to the observations, capturing the spatial details as well as the seasonal variation, even though the model tends to overestimate the precipitation amount regardless of the season. When comparing the mother domain with the station observation, its spatial details appear to be coarse. Overall, the nested domain simulation shows a good agreement with the observations in both seasonality and spatial details. The comparison of temperature across the different resolutions presents a similar behavior, reflecting the topographical forcing (not shown). This result provides evidence that the fine scale details are better resolved in nested domain simulation, which justifies the need for high resolution modeling over the region.

As a verification of daily properties, wet and dry spells in terms of the sequences of wet and dry days over various durations are analyzed using the daily precipitation (Fig. 8). A wet day is defined as a day with precipitation accumulation greater than or equal to 1.0 mm (Im and Kwon, 2007). At least

one wet day is referred to as a wet spell. Wet and dry spells are divided into 11 duration intervals, each of which is empirically chosen based on the expected properties of the weather variables, as the interval size gradually increases. Figure 8 describes the annual frequency distribution of dry and wet spells of various durations between the observation and reference simulation. For comparison between dry and wet spells, the shapes of the two distributions are quite different, indicating that dry spells exhibit a much longer duration than the wet ones. The model reproduces dry spell characteristics of the relative ratio of the frequencies across various durations. In contrast to the dry spells, the model reveals an overestimation in the wet spells, which is amplified as the duration lengths become longer. The model tends to produce an excessive occurrence of weak precipitation indicating an overestimation of frequency; therefore, the decreasing ratio of simulated frequency in the long-duration period shows a more gently gradient than the observation. This is a commonly raised problem in the precipitation performance of climate modeling (Frei *et al.*, 2003). In spite of this limitation, the model appears to properly simulate the characteristics of daily precipitation. Furthermore, Im *et al.* (2011) demonstrate the reasonable performance of the same simulation for capturing the temporal and spatial structure of the frequency and intensity of heavy precipitation.

Figure 9 presents the time series of annually averaged temperature and precipitation anomalies over Korea throughout the entire integration period from the nested domain simulation. It

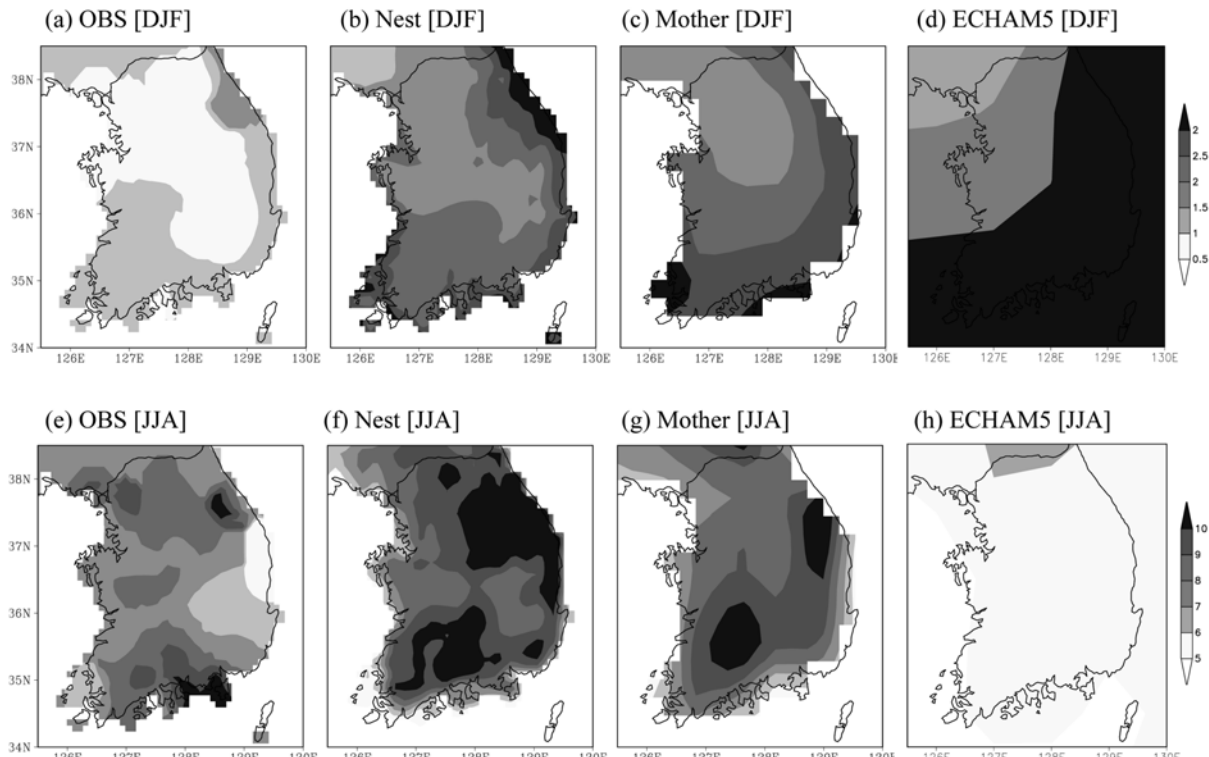


Fig. 7. Spatial distribution of precipitation averaged over 30 years for winter (a, b, c, and d) and summer (e, f, g, and h). Here, (a) and (e) correspond to the 57 station observation, (b) and (f) to the nested domain simulation, (c) and (g) to the mother domain, and (d) and (h) are the results from the ECHAM5 simulations. Units are mm d^{-1} .

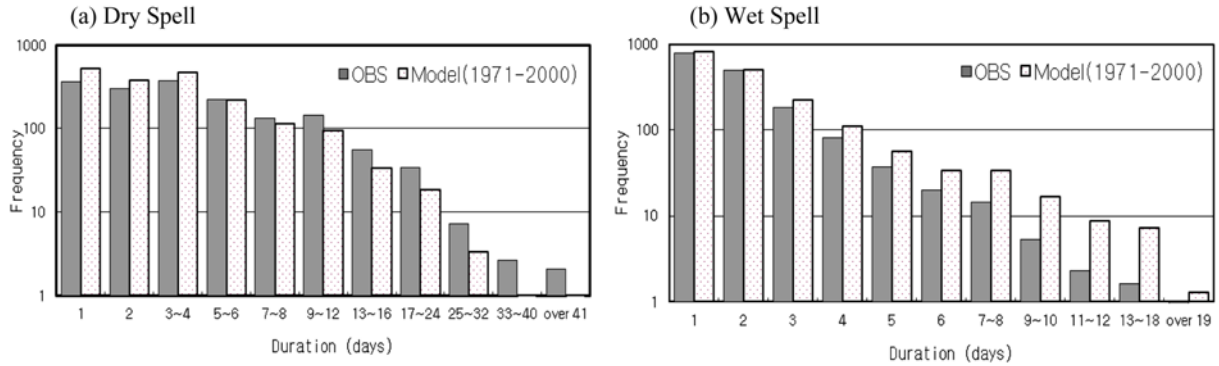


Fig. 8. Frequency distribution of (a) dry and (b) wet spells across various durations derived from observed and simulated daily precipitation over Korea. Here, a wet day is defined as a day with precipitation accumulation greater than or equal to 1.0 mm. The y-axis denotes a logarithmic scale.

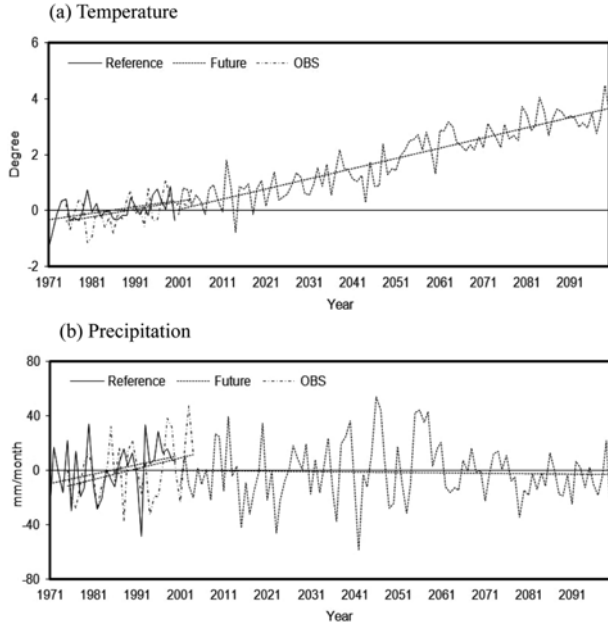


Fig. 9. Annually averaged (a) temperature and (b) precipitation anomalies with respect to the reference period (OBS: 1975-2004, Model: 1971-2000) over Korea.

Table 1. Summary of basic statistics derived from Fig. 9 during the reference period (OBS: 1975-2004, Model: 1971-2000). Here, the units of temperature and precipitation are $^{\circ}\text{C}$ and mm mo^{-1} , respectively.

	Mean		Standard Deviation		Trend (per 30-yr)	
	OBS	REF	OBS	REF	OBS	REF
Temperature	12.43	12.16	0.54	0.46	0.83	0.70
Precipitation	111.97	140.23	21.76	19.92	23.80	20.45

provides useful insight into the trend and persistency in the long-term variability of the climate change signal in response to increasing GHG concentration. To validate the simulated results during the reference period (1971-2000), we also display the observed estimates archived at the Korean climate stations (averaged over 57 locations, 1975-2004). The mean, variability, and trends of the simulated temperature and precipitation

demonstrate similarity with those of the observations, in spite of the overestimation of the mean precipitation (Table 1). The temperature shows a gradually increasing pattern. The precipitation also exhibits an overall increase, but it has large interannual and interdecadal variability. According to the projection for the twenty-first century, the degree of warming is sharply accelerated, indicating a well-defined increasing trend. The temperature is projected to increase continuously up to 4°C at the end of the twenty-first century. The projected change of precipitation is different, however. When viewed in the context of the whole twenty-first century, it is difficult to find any readily apparent trends in the precipitation evolution. However, since the trend depends on the selected period, for certain periods (e.g., 2021-2040) there is a visibly increasing trend while a decreasing pattern is discernible after the 2050s. This implies that projections derived for a short future period could produce erroneous interpretation of the results because the projected change could be skewed by unrecognized forced variability (e.g., interdecadal variability).

Changes in temperature and precipitation characteristics are attributed to the moisture budget. The increase or decrease of precipitation can be the root cause of moisture surplus or deficit in the atmosphere, and the increase of temperature can also control the atmospheric moisture demand through evapotranspiration (Easterling *et al.*, 2007). Using the monthly temperature and precipitation data, we calculate the PDSI for the whole integration period (130-year) in order to measure the evolution of drought conditions. Figure 10 describes the monthly PDSI averaged over 57 stations in Korea, and their trends derived from the observation (1975-2004) and simulations (Reference: 1971-2000 and Future: 2001-2100). Comparing the similarity between the observed and simulated temporal structure of the temperature and precipitation (Fig. 9), the PDSI from the model is able to realistically capture the characteristics, in terms of the direction and magnitude of the trend during the reference period. The PDSI shows a tendency to increase with increasing precipitation. There is also general phase coherence between the PDSI and precipitation variation, because 70-90% (10-30%) of the PDSI's variances are modulated by variances in precipitation (temperature; Dai *et al.*, 2004).

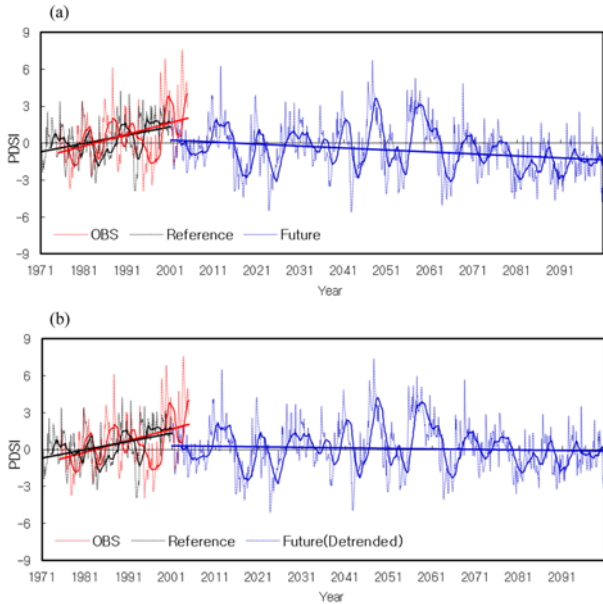


Fig. 10. Time-series of the PDSI (dotted line), 25-month moving average (thick line), and its trend (thick linear line) derived from the observation (red color), reference simulation (black color), and future simulation (blue color) with (a) original and (b) detrended temperatures. Here, the time-series of the PDSI derived from the observation and reference simulation are the same as those in (a) and (b).

The future behavior of the PDSI exhibits different behavior. In view of the long-term trend covering the entire twenty-first century, the relevant decline of the PDSI is visible (Fig. 10a). Although the variation of the PDSI is mostly associated with the precipitation, it is difficult to detect a meaningful trend in the precipitation time-series (Fig. 9b). Therefore, the downward trend in the temporal evolution of the PDSI tends to be modulated by the temperature (See the explanation of Fig. 12).

To investigate the regional dependence and statistical signifi-

cance of the PDSI trends, we perform the Mann-Kendall statistical test based on individual stations over Korea (Fig. 11). The Mann-Kendall test is one of the widely used non-parametric tests to detect significant trends in time series data (Mann, 1945; Kendall, 1975). During the reference period, both the observation and simulation show increasing trends across whole areas (except for 4 stations in the model). Most of the trends at the station locations are statistically significant at the 95% confidence level. The model follows well the observed estimates, but areas of opposite sign and lower significance are found over the northwest part of South Korea. Moving to the future projection, the directions of the trends are completely altered in our simulation. Except for several stations along the southern coastal area, the majority of stations shows decreasing trends with high statistical significance.

This change in trend can be attributed to the precipitation decrease and/or temperature increase. Even though there is no significant trend in precipitation during the whole period, a negative anomaly in precipitation is dominant in the latter part of the twenty-first century. Also, the positive trends along the south coast directly reflect the precipitation effect because this region is not affected by any summer precipitation decrease (Fig. 6d). Next, the trend for a large increase in temperature could be an additional contributor to the future dryness as measured by the PDSI. An increased temperature enhances evapotranspiration, and thus increases moisture flux from the surface to the atmosphere (Boo *et al.*, 2004). By comparison with the reference simulation, the much faster increasing rate of temperature is more responsible for the future dryness accompanying the enhancement of atmospheric water demand.

To demonstrate the effect of increasing temperature on the PDSI change quantitatively, we calculate the PDSI using the detrended temperature time-series (Fig. 10b). The linear trend, obtained from a least square fit line to the whole integration period, is removed from the monthly temperature time series.

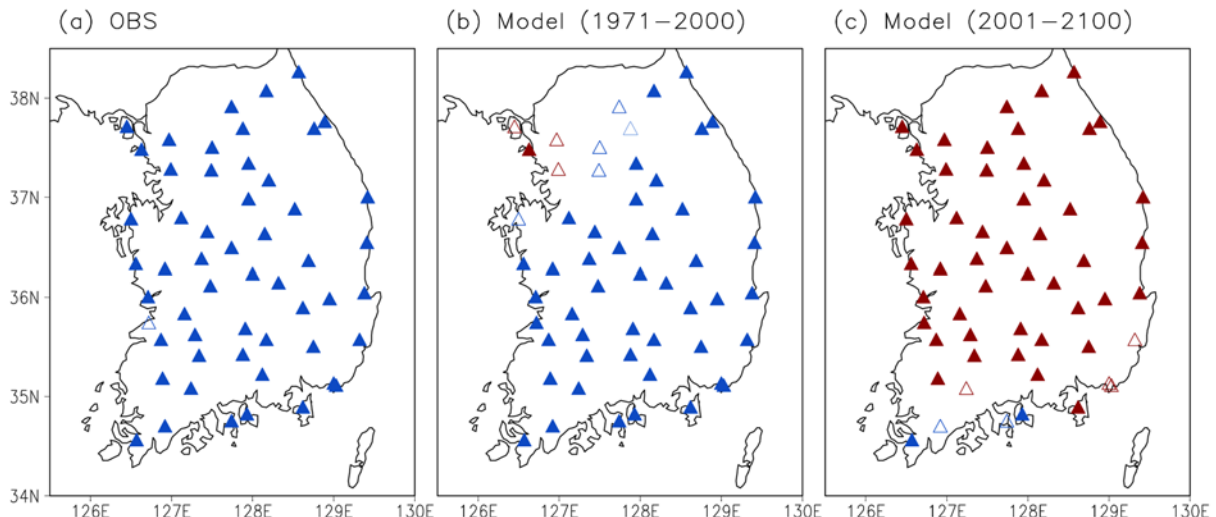


Fig. 11. Spatial distribution of the PDSI trends derived from (a) observation, (b) reference and (c) future simulation over Korea. Here, the blue and red colors indicate the upward and downward trends, respectively. The closed triangles are significant at the 0.05 significance level from the Mann-Kendall statistical test.

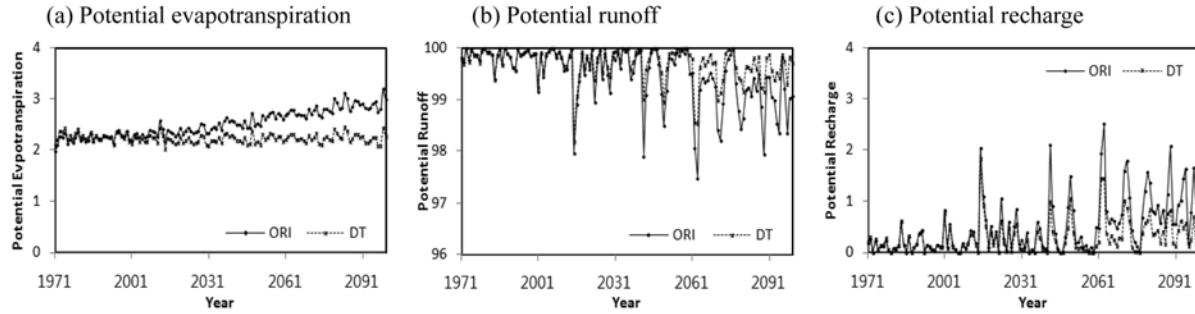


Fig. 12. Time-series of potential evapotranspiration, potential runoff, and potential recharge derived from two cases of PDSI calculations. Here, ORI (DT) denotes the case of original (detrended) temperatures as an input for PDSI.

The monthly precipitation amount is the same as that used for the calculation of Fig. 10a. While the PDSI derived from the detrended temperature time-series (Fig. 10b) shows a similar temporal variation to that of Fig. 10a, the decreasing trend has mostly disappeared. This suggests that the climatic long-term trend of drought tends to be modulated by the temperature trend, even though the variation of drought is mainly determined by the change of precipitation. A consistently increasing trend of temperature could accelerate the relative departure of moisture from its climatological condition. Considering the high confidence that temperature will continue to increase in response to emission forcing, it is likely that the future climate will be more favorable for dryness condition.

To calculate the PDSI, the important value is the departure of moisture from its climatological condition, and it is determined by the excess or shortage of precipitation compared to the climatological precipitation appropriate for existing conditions. Figure 12 displays the temporal evolution of potential evapotranspiration, potential runoff, and potential recharge, which are the main variables in determining the potentially available moisture condition in the PDSI computation. The difference of potential evapotranspiration derived from the original (ORI in Fig. 12) and detrended (DT in Fig. 12) temperature time series clearly represents the impact of the temperature. In case of using the detrended temperature as an input for PDSI, the potential evapotranspiration does not exhibit any trend corresponding to the temperature. Once evapotranspiration increases, more moisture is deprived from the available soil moisture, which reduces the potential runoff. The behavior of potential recharge seems to mirror potential runoff because, if the potential recharge is increased by absorption of soil, this in turn reduces the potential runoff. Therefore, both of them appear to be balanced in the average sense during the analysis period in contrast to the predominant increasing trend of evapotranspiration. As a result, further increase of moisture demand for the enhanced evapotranspiration induces a more pronounced actual water stress under the warmer climate condition.

4. Summary and discussion

To estimate the potential future changes in the dryness over

Korea, we have analyzed the dynamically downscaled ECHAM5 A1B projection using the RegCM3 double-nested system. A 130-year long simulation was performed, and the general feature over East Asia from the mother domain simulation and detailed structure over Korea from the nested domain simulation have been discussed.

The East Asia mean changes in temperature and precipitation derived from the ECHAM5 global projection are in line with those found in other CMIP3 participant models. However, when examined on the regional scale, it projects a decrease of summer precipitation over Korea, which is rather different from the ensemble mean. The general feature of the ECHAM5 projection tends to be inherited by downscaled regional pattern. To reduce the uncertainty range, there is a need for further ensemble experiments forced by multi-GCM projections.

For the mother domain simulation during the reference period (1971–2000), the model reasonably reproduces the mean climatology of the temperature and precipitation in terms of the seasonal variation and spatial distribution as seen in the CRU observed patterns. For future change, the temperature is projected to increase in all seasons over the entire region. Warming is reaching over 4°C, with a different geographical location of maximum warming in the cold and warm seasons. The change of precipitation shows a distinct seasonal variation. Moreover, pronounced regional differences are observed in the simulation and the statistical significant regions are also restricted due to large natural variability.

The validation against a dense observational station over Korea demonstrates that the nested domain simulation improves the spatial distribution of surface variables due to a better representation of relevant geographical features, and shows reasonable performance of daily characteristics. For the temporal evolution of the simulated temperature and precipitation averaged over Korea, the mean, variability, and trends show similarity with those of the observations. The changes in temperature and precipitation alter the budget of soil moisture. We attempt to examine this feature based on the PDSI estimation using the nested domain simulation. During the reference period, the variability and trend of PDSI calculated from monthly temperature and precipitation time-series are in good agreement with the observed estimates corresponding to the temperature and precipitation. The PDSI tends to follow the

precipitation variation, and both the observed and simulated patterns during the reference period show overall increasing trends with statistical significance at the 95% confidence level. However, the relevant decline of the PDSI is visible in the future projection, which is attributed to the combined effect of precipitation and temperature. Even though the changes in total precipitation do not show any relevant trend over the entire period, it is evident that the precipitation amount as well as the variability are reduced after the 2050s. Next, the much faster future increasing rate of temperature is more responsible for the PDSI decreasing trend compared to the reference period. The relationship between global warming and the PDSI is actually complicated and nonlinear, but one plausible explanation is related to the effect of the temperature trend in modulating the climatic long-term trend of the PDSI. Such an effect is supported by the fact that the downward trend of the PDSI mostly disappears when the detrended temperature is used to calculate the PDSI. It should be noted that although drought is generally associated with precipitation amount, an increase or decrease of the total precipitation does not necessarily mean more or less intense drought conditions. For example, an increase of total precipitation due to the contribution of heavy precipitation would not be helpful for reducing drought. On the contrary, extreme precipitation can be significantly enhanced without increasing the total precipitation as in our projection (Im *et al.*, 2011). Therefore, it's not enough to estimate the future dryness based on long-term averaged precipitation (e.g., monthly or seasonal temporal scale). Systematic investigations of short-duration precipitation and combined effect with temperature are needed to understand the accurate characteristics of the hydroclimatic change due to global warming.

Acknowledgements. The authors wish to thank the two anonymous reviewers and editor whose valuable comments and suggestions greatly improved the quality of this paper. This work was funded by the Korea Meteorological Administration Research and Development Program under Grant RACS_2010-4012. This work was also partially supported by a grant (code#3100-3136-442) funded by the National Institute of Meteorological Research (NIMR), the Korea Meteorological Administration (KMA).

Edited by: John McGregor

REFERENCES

- Andreadis, K. M., and D. P. Lettenmaier, 2006: Trends in 20th century drought over the continental United States. *Geophys. Res. Lett.*, **33**, L10403, doi:10.1029/2006GL025711.
- Boo, K.-O., W.-T. Kwon, J.-H. Oh, and H.-J. Baek, 2004: Response of global warming on regional climate change over Korea: An experiment with the MM5 model. *Geophys. Res. Lett.*, **31**, L21206, doi:10.1029/2004GL021171.
- Cha, Y.-M., H.-S., W.-T. Kwon, and K.-O. Boo, 2007: Impacts of the land-sea distribution around Korean Peninsula on the simulation of East Asia summer precipitation. *Atmosphere*, **17**, 241-253. (In Korean with English abstract)
- Chow, K. C., J. C. L. Chan, J. S. Pal, and F. Giorgi, 2006: Convection suppression criteria applied to the MIT cumulus parameterization scheme for simulating the Asian summer monsoon. *Geophys. Res. Lett.*, **33**, L24709, doi:10.1029/2006GL028026.
- Coppola, E., and F. Giorgi, 2009: An assessment of temperature and precipitation change projections over Italy from recent global and regional climate model simulations. *Int. J. Climatol.*, **30**, doi:10.1002/joc.1867.
- Dai, A., K. E. Trenberth, and T. Qian, 2004: A global dataset of Palmer Drought Severity Index for 1870-2002: Relationship with soil moisture and effects of surface warming. *J. Hydrometeor.*, **5**, 1117-1130.
- Dickinson, R. E., A. Henderson-Sellers, and P. J. Kennedy, 1993: Biosphere- Atmosphere Transfer Scheme (BATS) version 1 as coupled to the NCAR community climate model. NCAR Technical Note NCAR/TN-387+STR, 72 pp.
- Dubrovsky, D., M. D. Svoboda, M. Trnka, M. J. Hayes, D. A. Wilhite, Z. Zalud, and P. Hlavinka, 2008: Application of relative drought indices in assessing climate-change impacts on drought conditions in Czechia. *Theor. Appl. Climatol.* doi:10.1007/s00704-008-0020-x.
- Easterling, D. R., T. W. R. Wallis, J. H. Lawrimore, and R. R. Heim, 2007: Effects of temperature and precipitation trends on U. S. drought. *Geophys. Res. Lett.*, **34**, L20709, doi:10.1029/2007GL031541.
- Emanuel, K. A., 1991: A scheme for representing cumulus convection in large-scale models. *J. Atmos. Sci.*, **48**, 2313-2335.
- Frei, C., J. H. Christensen, M. Deque, D. Jacob, R. G. Jones, and P. L. Vidale, 2003: Daily precipitation statistics in regional climate models: Evaluation and intercomparison for the European Alps. *J. Geophys. Res.*, **108(D3)**, 4124, doi:10.1029/2002JD002287.
- Gao, X., Y. Shi, R. Song, F. Giorgi, Y. Wang, and D. Zhang, 2008: Reduction of future monsoon precipitation over China: comparison between a high resolution RCM simulation and the driving GCM. *Meteor. Atmos. Phys.*, **100**, 73-86.
- Giorgi, F., and Coauthors, 2009: The regional climate change Hyper-Matrix Framework. *EOS*, **89**, 445-456.
- Hagemann, S., H. Gottel, D. Jacob, P. Lorenz, and E. Roeckner, 2009: Improved regional scale processes reflected in projected hydrological changes over large European catchments. *Climate Dyn.*, **32**, 767-781.
- Holtslag, A. A. M., E. I. F. de Bruijin, H. L. Pan, 1990: A high resolution air mass transformation model for short-range weather forecasting. *Mon. Wea. Rev.*, **118**, 1561-1575.
- Im, E.-S., E.-H. Park, W.-T. Kwon, and F. Giorgi, 2006: Present climate simulation over Korea with a regional climate model using a one-way double-nested system. *Theor. Appl. Climatol.*, **86**, 187-200.
- _____, and W.-T. Kwon, 2007: Characteristics of extreme climate sequences over Korea using a regional climate scenario. *SOLA*, **3**, 17-20.
- _____, _____, J.-B. Ahn, and F. Giorgi, 2007: Multi-decadal scenario simulation over Korea using a one-way double-nested regional climate model system. Part 1: recent climate simulation (1971-2000). *Climate Dyn.*, **28**, 759-780.
- _____, _____, _____, and _____, 2008a: Multi-decadal scenario simulation over Korea using a one-way double-nested regional climate model system. Part 2: future climate projection (2021-2050). *Climate Dyn.*, **30**, 239-254.
- _____, J.-B. Ahn, A. R. Remedio, and W.-T. Kwon, 2008b: Sensitivity of the regional climate of East/Southeast Asia to convective parameterization in the RegCM3 modeling system. Part 1: Focus on the Korean peninsula. *Int. J. Climatol.*, **28**, 1861-1877.
- _____, and _____, 2011: On the elevation dependency of present-day and future climate simulations from a high-resolution regional climate model. *J. Meteorol. Soc. Japan*, **89**, 89-100.
- _____, I.-W. Jung, and D.-H. Bae, 2011: The temporal and spatial

- structure of recent and future trends in extreme indices over Korea from a regional climate projection. *Int. J. Climatol.*, doi:10.1002/joc.2063.
- International Panel on Climate Change (IPCC), 2007: The Physical Science Basis. Contribution of Working Group I to the Fourth Assessment Report of the Intergovernmental Panel on Climate Change. Solomon, S., D. Qin, M. Manning, Z. Chen, M. Marquis, K.B. Averyt, M. Tignor and H.L. Miller (eds.). Cambridge Univ. Press, 996 pp.
- Karnauskas, K. B., A. Ruiz-Barradas, S. Nigam, and A. J. Busalacchi, 2008: North American droughts in ERA-40 global and NCEP North American regional reanalyses: A Palmer Drought Severity Index perspective. *J. Climate*, **21**, 2102-2123.
- Kendall, M. G., 1975: Rank Correlation Methods, Charles Griffin, London.
- Kiehl, J. T., J. J. Hack, G. B. Bonan, B. A. Boville, B. P. Briegleb, D. L. Williamson, and P. J. Rasch, 1996: Description of NCAR Community Climate Model (CCM3). NCAR Technical Note NCAR/TN-420+STR, 152.
- Kim, D.-W., and H.-R. Byun, 2009: Future pattern of Asian drought under global warming scenario. *Theor. Appl. Climatol.*, doi:10.1007/s00704-008-0100-y.
- Kripalani, R. H., J.-H. Oh, and H. S. Chaudhari, 2007: Response of the East Asian summer monsoon to doubled atmospheric CO₂: Coupled climate model simulations and projections under IPCC AR4. *Theor. Appl. Climatol.*, **87**, 1-28.
- Mann, H. B., 1945: Nonparametric tests against trend, *Econometrica*, **13**, 245-259.
- New, M. G., M. Hulme, and P. D. Jones, 2000: Representing twentieth century space time climate fields. Part II. Development of a 1901-1996 mean monthly terrestrial climatology. *J. Climate*, **13**, 2217-2238.
- Pal, J.-S., and Coauthors, 2007: The ICTP RegCM3 and RegCNET: regional climate modeling for the developing world. *Bull. Amer. Meteor. Soc.*, **88**, 1395-1409.
- Park, E.-H., S.-Y. Hong, and H.-S. Kang, 2008: Characteristics of an East-Asian summer monsoon climatology simulated by the RegCM3. *Meteor. Atmos. Phys.*, **100**, 139-158.
- Wells, N., S. Goddard, and M. J. Hayes, 2004: A self-calibrating Palmer Drought Severity Index. *J. Climate*, **17**, 2335-2351.